RadioGraphics

Cardiac MR Imaging and MR Angiography for Assessment of Complex Tetralogy of Fallot and Pulmonary Atresia[1]

M. Ines Boechat, MD • Osman Ratib, MD, PhD • Penny L. Williams, MD • Antoinette S. Gomes, MD • John S. Child, MD • Vivekanand Allada, MD

ONLINE-ONLY CME

See www.rsna.org/education/rg_cme.html.

LEARNING OBJECTIVES

After reading this article and taking the test, the reader will be able to:

- Describe the developmental abnormality that leads to tetralogy of Fallot.
- Identify the MR pulse sequences used to evaluate cardiac function, morphologic features, and three-dimensional anatomy in patients suspected of having tetralogy of Fallot.
- Discuss the cardiac MR features of tetralogy of Fallot, including the spectrum of pulmonary artery morphologic features, associated findings, and pre- and postoperative appearances.

Breath-hold electrocardiographically gated cardiac magnetic resonance (MR) imaging and contrast material–enhanced MR angiography are emerging as ideal techniques for the evaluation of complex congenital heart disease. Tetralogy of Fallot is the most common cause of cyanotic congenital heart disease and, in its classic form, is associated with varying degrees of hypoplasia of the central and peripheral pulmonary arteries, with valvar pulmonary atresia and collateral aortopulmonary vessels occupying the extreme end of the spectrum. Accurate assessment of the size and anatomy of the pulmonary arteries is often difficult with echocardiography and conventional cineangiography. Compared with echocardiography in particular, cardiac MR imaging with three-dimensional reconstruction has distinct advantages for pre- or postoperative assessment of pulmonary anatomy in patients with tetralogy of Fallot and pulmonary atresia. MR imaging enables the clear and complete depiction of anatomy and thus can provide additional information about pulmonary artery abnormalities that are difficult to evaluate with conventional cardiac imaging techniques.

Abbreviations: ECG = electrocardiography, SE = spin echo, 3D = three-dimensional

RadioGraphics 2005; 25:1535–1546 • **Published online** 10.1148/rg.256045052 • **Content Codes:** MR PD

[1]From the Department of Radiological Sciences (M.I.B., O.R., P.L.W., A.S.G.), Department of Pediatrics (V.A.), and Division of Cardiology (J.S.C.), University of California at Los Angeles, David Geffen School of Medicine, 650 Charles E. Young Dr S, Box 951721, Los Angeles CA 90095-1721. Recipient of Certificate of Merit and Excellence in Design awards for an education exhibit at the 2002 RSNA Annual Meeting. Received March 24, 2004; revision requested June 3 and received April 4, 2005; accepted April 18. All authors have no financial relationships to disclose. **Address correspondence to** M.I.B. (e-mail: *iboechat@mednet.ucla.edu*).

Introduction

Tetralogy of Fallot is among the most common cyanotic heart diseases in children and accounts for approximately 4%–8% of all congenital cardiac lesions. It is the consequence of a single developmental abnormality, the misalignment of the crista supraventricularis with associated underdevelopment of the infundibulum. This abnormality results in ventricular septal defect, anterior displacement of the aortic valve, right ventricular outflow tract obstruction, and consequent right ventricular hypertrophy (1,2). Depending on the degree of obstruction of the right ventricular outflow tract, bronchial and aortopulmonary collateral vessels may supply a variable amount of blood to the lungs. Tetralogy of Fallot is often associated with pulmonary artery atresia of various degrees of severity (from mild arterial hypoplasia to the complete absence of the main pulmonary artery or the nonconfluence of its branches). Other commonly associated anomalies are right-sided aortic arch, which is present in 25% of cases, and atrial septal defect, which is present in approximately 5% of cases. Ventricular septal defect, persistent left superior vena cava, coronary artery abnormalities, and aberrant right subclavian artery also have been noted. Rarely, tracheoesophageal fistula, rib anomalies, and scoliosis are present.

With regard to clinical symptoms, cyanosis usually develops by the age of 3–4 months, but the time of manifestation depends on the degree of right ventricular outflow tract obstruction. Dyspnea during physical exertion and adoption of a squatting position are typical clinical signs used for diagnosis in older children and adults.

The features of tetralogy of Fallot observed at conventional imaging are well known: Plain radiographs show a normal-sized to slightly enlarged cardiac silhouette. The ventricular apex is often upturned, and the main pulmonary artery segment appears concave. This classic combination of features gives the heart the appearance of a boot. Modern imaging techniques allow early diagnosis and treatment (3). Currently, most patients with tetralogy of Fallot undergo a modified Blalock-Taussig procedure in infancy if necessary and complete surgical correction around 1 year of age. Adults with uncorrected tetralogy of Fallot are rarely encountered.

The article describes the benefits of cardiac magnetic resonance (MR) imaging with three-dimensional (3D) reconstruction for pre- and postoperative evaluation of the pulmonary vascular anatomy in pediatric patients with tetralogy of Fallot and pulmonary atresia, as well as for follow-up evaluation of the anatomy in adult patients many years after surgery.

Cardiac MR Imaging Techniques

MR imaging provides anatomic and functional information that is superior to that provided by conventional cardiac imaging modalities such as echocardiography and angiography. Contrast material–enhanced MR angiography is particularly useful for the assessment of deep anatomic structures such as the pulmonary arteries, which are difficult to see on echocardiograms and difficult to access at selective angiography. Furthermore, cine MR images can provide additional information about cardiac function, valve patency, and the hemodynamic significance of vascular stenosis.

Morphologic Assessment

The high spatial resolution and high image contrast required for adequate morphologic assessment of cardiac structures and thoracic vessels can be obtained by using electrocardiographically (ECG) gated T1-weighted spin-echo (SE) MR imaging sequences. Images obtained with these sequences, however, may be affected by respiratory motion artifacts, even if they are obtained with averaging of multiple signals and a long echo time at the cost of longer acquisition times. Fast SE and turbo SE techniques reduce acquisition time considerably but are vulnerable to the same type of motion artifact. Dark-blood–prepared turbo SE sequences are commonly used in conjunction with breath-hold turbo SE sequences. Fast imaging sequences that are more robust with regard to motion artifacts are half-Fourier rapid acquisition with relaxation enhancement (turbo SE) sequences with dark-blood preparation, which are much less vulnerable to motion-related artifacts because of the short acquisition time. Since the development of fast imaging with steady-state precession, it is also possible to acquire a stack of single-shot anatomic images with short breath-hold times that provides a detailed anatomic and topologic assessment of the heart and great vessels.

Functional Assessment

ECG-gated cine MR pulse sequences can be applied in any oblique plane along the cardiac chambers or great vessels to obtain images that are similar to echocardiographic images but with a higher spatial resolution and less limitation in plane positioning. Traditionally, functional evaluation of cardiac wall motion is performed by using ECG-gated gradient-echo techniques or segmented (fast) gradient-echo techniques. The resultant multiphase bright-blood images depict cardiac motion in multiple frames through the cardiac cycle. These dynamic images also provide additional information about blood flow patterns across the cardiac valves and deformed large vessels, where turbulence from regurgitation jets or

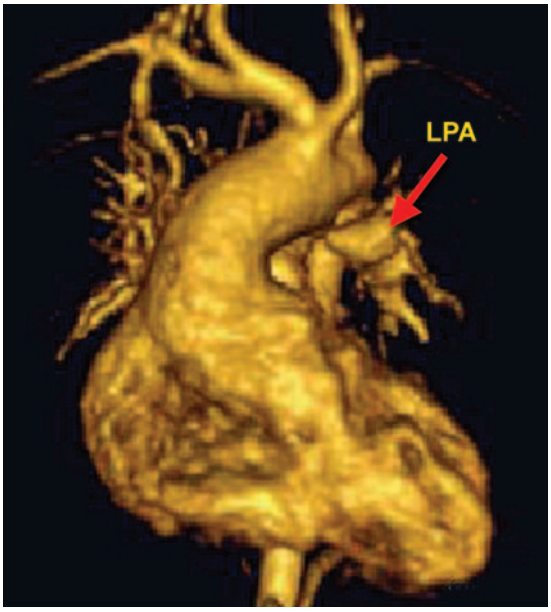

Figure 1. Anterior 3D volume-rendered MR image in the coronal plane shows pulmonary atresia and nonconfluence of the left pulmonary artery *(LPA)* with a blind right ventricular outflow tract.

disordered flow produces regions of signal void from dephased spins. The recently developed "ultrafast" sequences allow high temporal resolution and very rapid acquisition of dynamic ECG-gated images of the heart and great vessels. Several manufacturers have introduced segmented MR sequences for fast acquisition of high-contrast dynamic cardiovascular images.

Contrast-enhanced MR Angiography

With the progress in MR imager development and the ability to acquire 3D MR images within a single breath hold (or during the first passage of a bolus of contrast material), contrast-enhanced MR angiography has become the method of choice for visualization of the great vessels of the chest and abdomen. Imaging parameters and partition dimensions should be carefully adjusted to achieve the smallest possible voxel size while allowing sufficient spatial coverage of the target vessels within a single breath-hold acquisition. Imaging time can be decreased by using partial Fourier imaging, fewer partitions, fewer phase encoding steps, or a rectangular field of view.

Postprocessing and Volume Rendering

The acquisition of 3D data in contiguous slabs allows the reformatting of images in an oblique orientation. From the 3D data set from MR angiography, for example, it is possible to obtain two-dimensional images in any oblique plane across the volume of data. With the high target-to-background contrast on MR angiographic images, it is often desirable to vary the section thickness to obtain two-dimensional reformatted images from 3D data sets that contain the required anatomic structures. This is particularly true for angiographic data where, by increasing the thickness of the reconstructed orthogonal or oblique plane, one may obtain a better view of multiple vascular branches and their course. The maximum intensity projection technique is the simplest and most widely used technique for visualization of 3D MR angiography data. It is based on a simple algorithm of projecting all the data on to one plane by selecting the highest intensity data element (voxel) in the data set along the projection lines. The resulting image is similar in appearance to images obtained from traditional X-ray angiography. Because maximum intensity projection does not differentiate the front from the back, overlap between adjacent structures makes it difficult to visually appreciate the exact spatial location of a given structure. An alternative rendering technique called surface rendering introduces a degree of opacity and thus allows better perception of the anatomic structures proximal to the viewing point and obscuring of structures that are located behind them. The surface rendering technique requires a selection of a surface, or threshold, between the object of interest and the surrounding structures. More advanced rendering techniques rely on sophisticated combinations of transparency and opacity of different anatomic structures. Under the common rubric of volume rendering, there are a variety of sophisticated algorithms that assign different degrees of opacity and even different colors and textures to objects in the volume of interest.

Preoperative MR Imaging Appearance

Pulmonary Artery Anomalies

A vast spectrum of pulmonary artery abnormalities is seen in patients with tetralogy of Fallot. In mild cases, there is a ventricular septal defect and mild pulmonary valve stenosis, known as "pink" tetralogy, which may be asymptomatic. The opposite end of the spectrum consists of complete pulmonary artery atresia with absence of the main pulmonary arteries, also known as pseudotruncus arteriosus. In patients with this condition, systemic-pulmonary collateral vessels and a right-to-left shunt such as that present in ventricular septal defect are essential for survival (Fig 1).

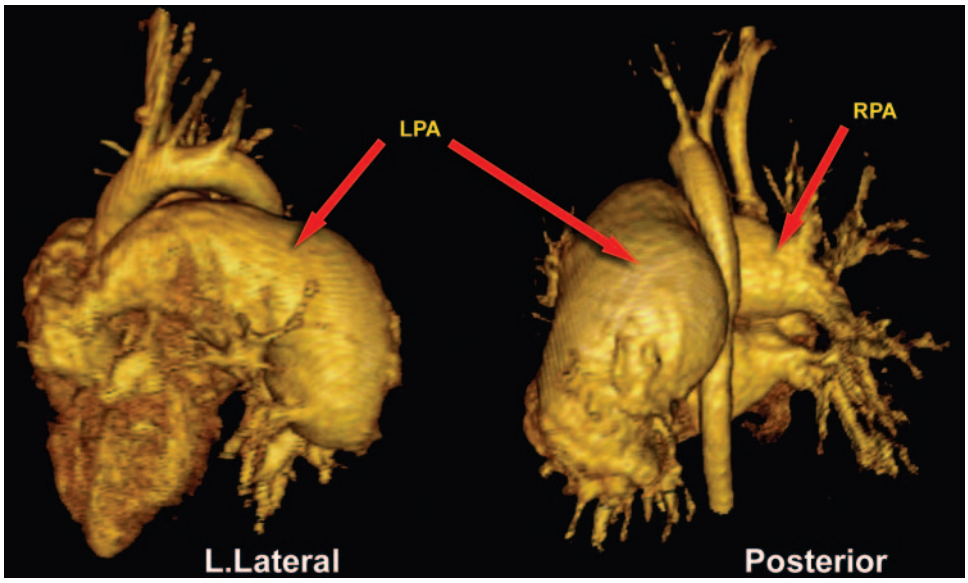

Figure 2. Left lateral and posterior coronal 3D volume-rendered MR images show aneurysmal dilatation of the left *(LPA)* and right *(RPA)* pulmonary arteries in an adult patient with uncorrected tetralogy of Fallot and severe pulmonary valve stenosis.

Pulmonary artery hypoplasia is associated with unilateral or segmental hypoplasia of the lungs, and both abnormalities are well depicted with MR imaging. The size and morphologic structure of the lungs may be assessed directly from the MR images, which complement the MR angiograms (4).

Postoperative survival has significantly improved, and an increasing number of patients who undergo surgery in childhood present for follow-up of late complications experienced in adulthood; MR is helpful in their diagnosis and in assessment of the appropriateness of reintervention. In adults with uncorrected tetralogy of Fallot, right ventricular hypertrophy often has developed to compensate for an increased pressure gradient across the narrow pulmonary outflow tract; eventually, however, the ventricle begins to fail and becomes dilated because of volume overload from regurgitation. In patients with severe pulmonary stenosis, aneurysmal dilatation of the pulmonary arteries may result from a postobstructive jet lesion. These conditions are well depicted with MR imaging (Fig 2).

Other Associated Anomalies

Several associated abnormalities found in patients with tetralogy of Fallot may influence surgical treatment planning in important ways. They include anomalies in the size and morphologic configuration of pulmonary arteries and in the presence and location of aortopulmonary collateral vessels, as well as pulmonary artery pruning (5–10).

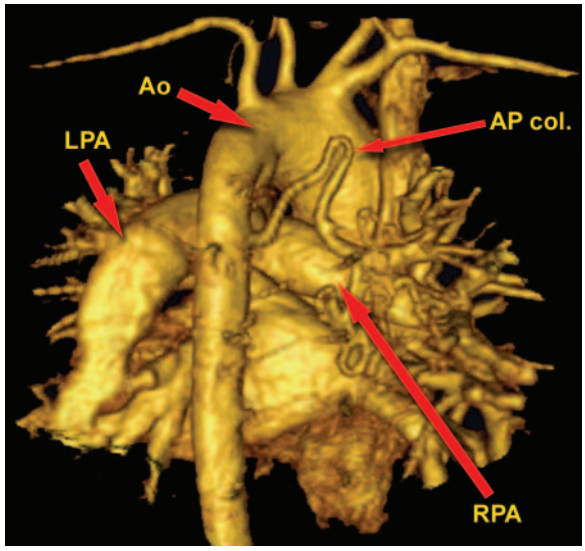

Figure 3. Posterior 3D volume-rendered MR image in the coronal plane shows an enlarged aortopulmonary collateral vessel *(AP col.)* supplying distal branches of the right pulmonary artery *(RPA)* in a patient with tetralogy of Fallot. *Ao* = aorta, *LPA* = left pulmonary artery.

A distinct advantage of cardiac MR imaging over echocardiography stems from its ability to depict distal pulmonary branches and delineate systemic-pulmonary collateral vessels, which are most visible on 3D volume-rendered images and reformatted images in oblique planes along the course of each vessel (Fig 3) (1,4,5,8,11–13).

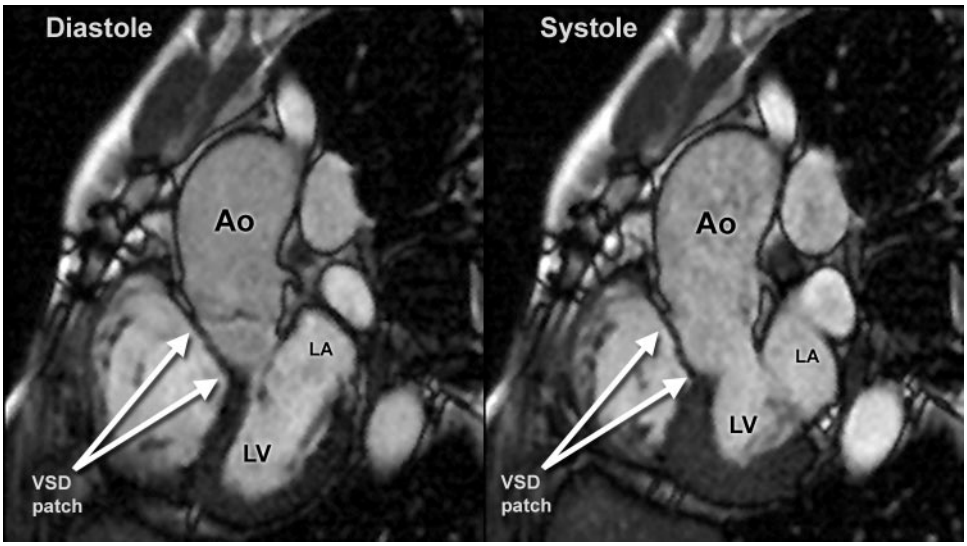

Figure 4. Dynamic cine MR images obtained in the short-axis plane at the level of the aortic outflow tract during diastole and systole show repair of a subaortic ventricular septal defect *(VSD patch)* and overriding aorta *(Ao)*. *LA* = left atrium, *LV* = left ventricle.

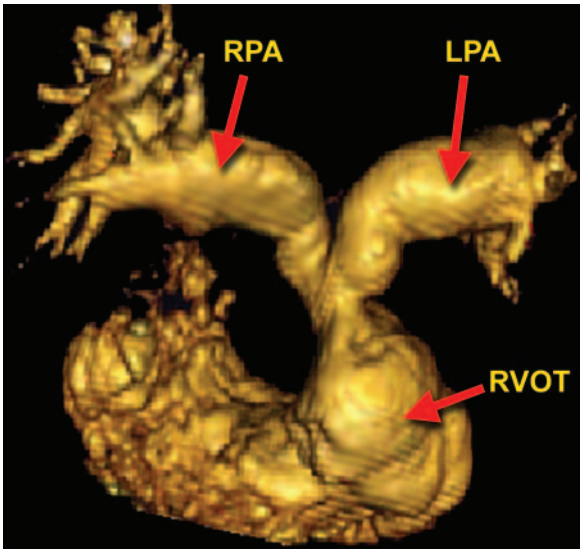

Figure 5. Anterior 3D volume-rendered image obtained in an adult patient 42 years after initial surgical repair of tetralogy of Fallot and reconstruction of hypoplastic pulmonary arteries shows enlarged right ventricular outflow tract *(RVOT)* and reconstructed right *(RPA)* and left *(LPA)* pulmonary artery branches with irregular shape but without significant narrowing or stenosis.

Echocardiography is limited by its poor ability to depict distal pulmonary artery segments, a limitation that results from the lack of an acoustic window that would allow the transmission of ultrasound waves through the air-filled lungs (1,4,6, 8,14).

Postoperative MR Imaging Appearance

Cardiac MR imaging techniques are especially useful for evaluating the postoperative anatomy. In general, the method of repair of tetralogy of Fallot depends on the patient's age, the degree of cyanosis, the extent of right ventricular outflow tract obstruction and pulmonary valve stenosis, the size of the ventricular septal defect, the presence and size of pulmonary arteries, and associated findings.

Currently, complete surgical correction of tetralogy of Fallot is the procedure of choice. Alternatively, a palliative technique such as the Blalock-Taussig shunt is applicable in infants who are not candidates for complete repair, and this procedure suffices until the pulmonary artery branches reach an age and size that permit complete repair. The modified Blalock-Taussig shunt allows blood to flow from a subclavian artery to the ipsilateral pulmonary artery via a synthetic tube.

Normal Postoperative Features

In most cases of tetralogy of Fallot, complete surgical repair involves reconstruction of the right ventricular outflow tract to eliminate the obstruction to pulmonary blood flow. Widening of the right ventricular outflow tract, closure of a ventricular septal defect (and atrial septal defect, if present) (Fig 4), and embolization of collateral aortopulmonary vessels are key steps in the procedure. Widening of the right ventricular outflow tract may be accomplished with or without patching of the infundibular tract by using pericardium or synthetic polyester fiber (Fig 5). In patients in whom widening of the native right ventricular

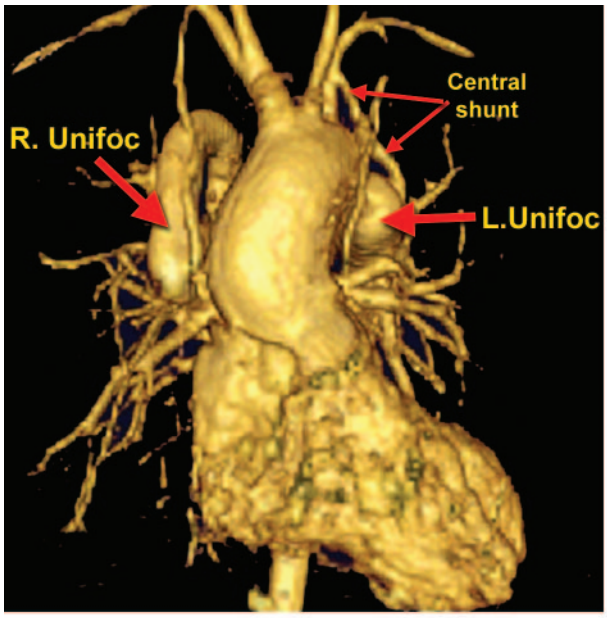

6.

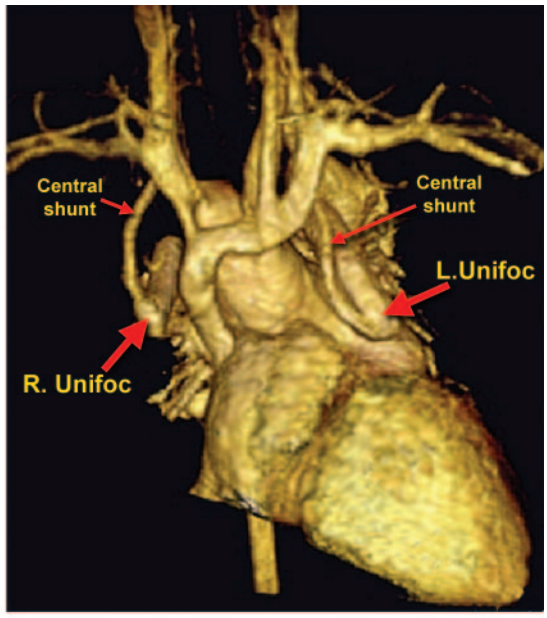

7.

Figures 6, 7. **(6)** Anterior 3D volume-rendered image, obtained after bilateral unifocalization in a patient with pulmonary atresia, shows anterior connection of the right unifocalization conduit *(R. Unifoc)* to the ascending aorta, and supply of the left unifocalization conduit *(L. Unifoc)* via a central shunt from the left subclavian artery. **(7)** Anterior 3D volume-rendered image obtained after bilateral unifocalization in a patient with pulmonary atresia and nonconfluent pulmonary arteries shows supply of both unifocalization conduits via central shunts from the respective subclavian arteries.

outflow tract is not feasible (eg, those with an anomalous coronary artery located in the region of the intended widening), a conduit from the right ventricle to the main pulmonary artery may be created that bypasses the obstruction (Rastelli procedure).

In the absence of one or both main pulmonary artery branches, the pulmonary blood supply can be rerouted by conjoining the bronchial and aortopulmonary collateral vessels into a single conduit supplied with systemic flow via an aortopulmonary shunt or a modified Blalock-Taussig shunt. This procedure, known as unifocalization, also involves the embolization and/or ligation of systemic collateral vessels. With this method, pulmonary artery pressures can be decreased to levels within the normal physiologic range. The shifting of the lung-directed blood flow from systemic vessels to pulmonary arteries protects the lungs from high systemic blood pressure and prevents vascular congestion and pulmonary hypertension (Figs 6, 7).

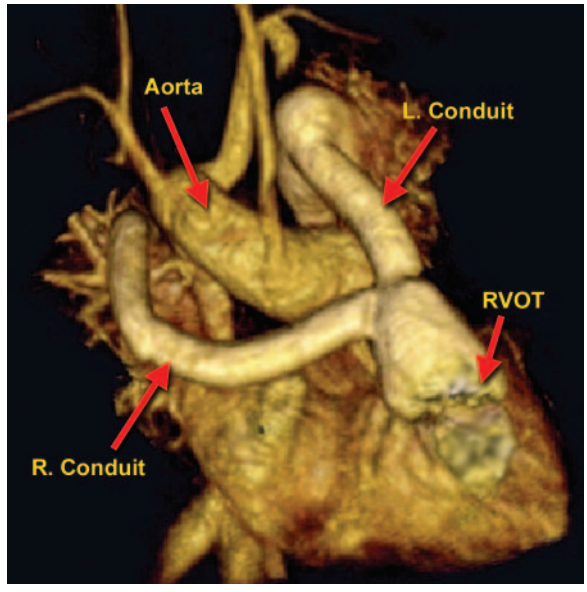

Figure 8. Anterior 3D volume-rendered image obtained after complete surgical repair of pulmonary atresia shows two prosthetic conduits that connect a reconstructed right ventricular outflow tract *(RVOT)* to the unifocalization chambers of the right *(R. Conduit)* and left *(L. Conduit)* pulmonary artery branches.

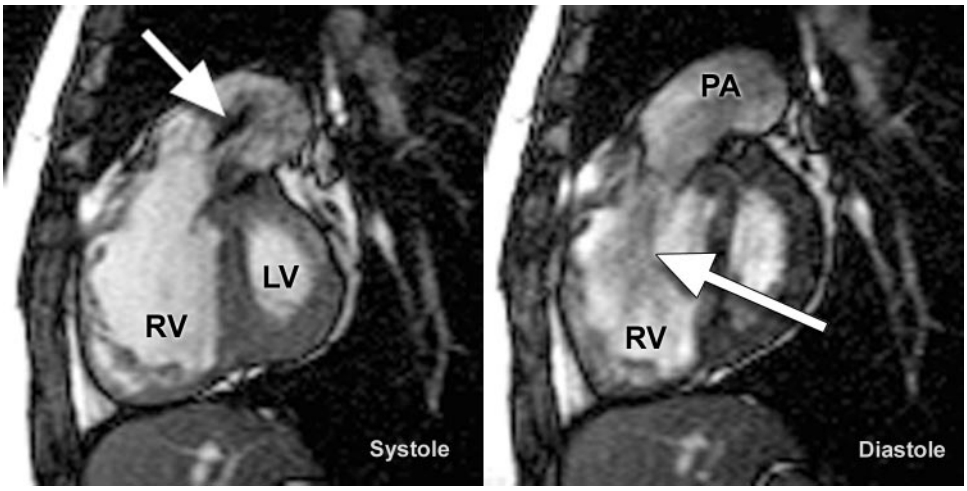

Figure 9. Dynamic cine MR images of the heart, obtained with a fast imaging with steady-state precession sequence, provide short-axis views at the level of the right ventricular outflow tract after surgical repair of tetralogy of Fallot. Residual valvular stenosis is indicated by a jet of low signal intensity during systole (left arrow) and by valvular regurgitation during diastole (right arrow). *LV* = left ventricle, *PA* = pulmonary artery, *RV* = right ventricle.

Complete surgical repair also is feasible with a single-step procedure or at a later stage of the patient's growth by connecting the two unifocalization tubes to the right ventricle via a Y-shaped conduit. The right ventricle may be connected to the pulmonary artery by means of a valvate conduit or, in patients with severe obstruction of the right ventricular outflow tract or pulmonary atresia, a nonvalvate conduit (Fig 8).

The value of MR imaging for postsurgical follow-up and planning of reintervention has been well demonstrated (15). The use of MR imaging for close monitoring of a decrease in right ventricular function, pulmonary artery regurgitation, and other functional parameters is possible and provides objective information for the postoperative evaluation of surgical repair (16).

Common Complications

Residual Stenosis.—A common complication of complete surgical repair is residual stenosis of the right ventricular outflow tract or pulmonary valve annulus. Residual stenosis may occur as the result of progressive scar tissue formation in the surgically repaired outflow tract (Fig 9). Alternatively, insufficient widening of the outflow tract at the time of surgical repair may result in a relative restriction of outflow after growth of the heart and great vessels.

Pulmonary Valve Regurgitation.—Significant pulmonary valve regurgitation is common after surgical repair and seems to become more significant as the patient grows older (Fig 9). Quantification of the regurgitation volume is possible with velocity-encoded cardiac MR imaging techniques, which allow accurate measurement of flow dynamics. Close monitoring of change in the extent of regurgitation over time is important for the prevention of progressive ventricular dysfunction and for planning of surgical repair before damage to the ventricle becomes irreversible (16).

Hypoplasia of Distal Pulmonary Arteries.—Despite increased blood supply to the distal pulmonary arteries after surgical repair of tetralogy of Fallot, they may receive insufficient stimulation for normal growth, a condition that leads to their underdevelopment and/or to that of the segmental pulmonary vessels (Figs 10, 11). The identification and localization of hypoplastic distal vessels may be critical for patient care and surgical decision making with regard to reintervention.

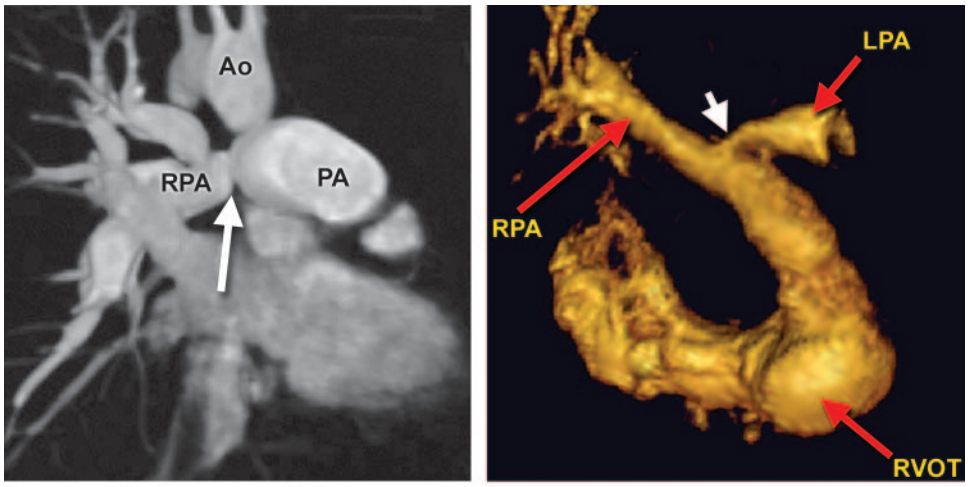

10. 11.

Figures 10, 11. **(10)** Coronal thick-slab reformatted image obtained with 3D MR angiography shows residual stenosis (arrow) at the origin of the right pulmonary artery *(RPA)* and the main pulmonary artery *(PA)* after surgical repair of tetralogy of Fallot. *Ao* = aorta. **(11)** Three-dimensional volume-rendered MR image of the origin of the left *(LPA)* and right *(RPA)* pulmonary arteries, obtained after patch enlargement of the right ventricular outflow tract *(RVOT)* in a patient with tetralogy of Fallot, shows segmental narrowing (white arrow) of the left pulmonary artery.

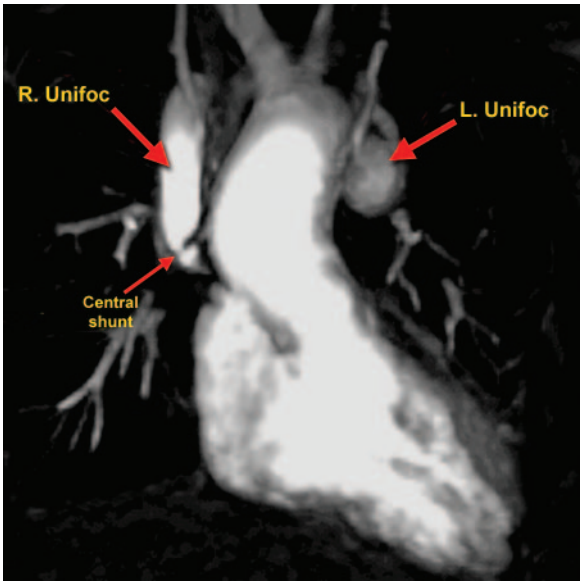

Figure 12. Coronal anterior thick-slab reformatted MR image shows bilateral unifocalization, with the right unifocalization conduit *(R. Unifoc)* connected to the ascending aorta via a short central shunt in which there is a mild-to-moderate segmental stenosis. *L. Unifoc* = left unifocalization conduit.

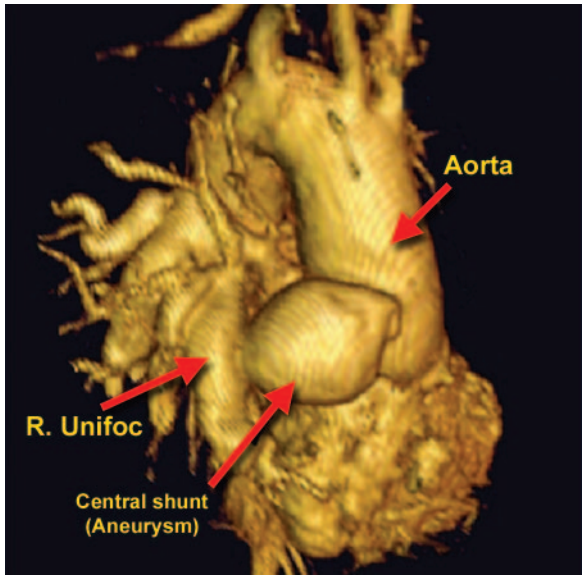

Figure 13. Right anterior oblique 3D volume-rendered MR image shows aneurysmal dilatation of a central shunt that connects a right unifocalization conduit *(R. Unifoc)* to the ascending aorta.

Obstruction or Stenosis of Central Shunts and Unifocalization Conduits.—MR imaging techniques are effective for evaluation of occluded or severely narrowed shunts or unifocalization conduits (Fig 12). It is critically important that stenosis be detected before the patient's clinical status deteriorates, because after deterioration occurs, it may be too late for effective intervention or revascularization.

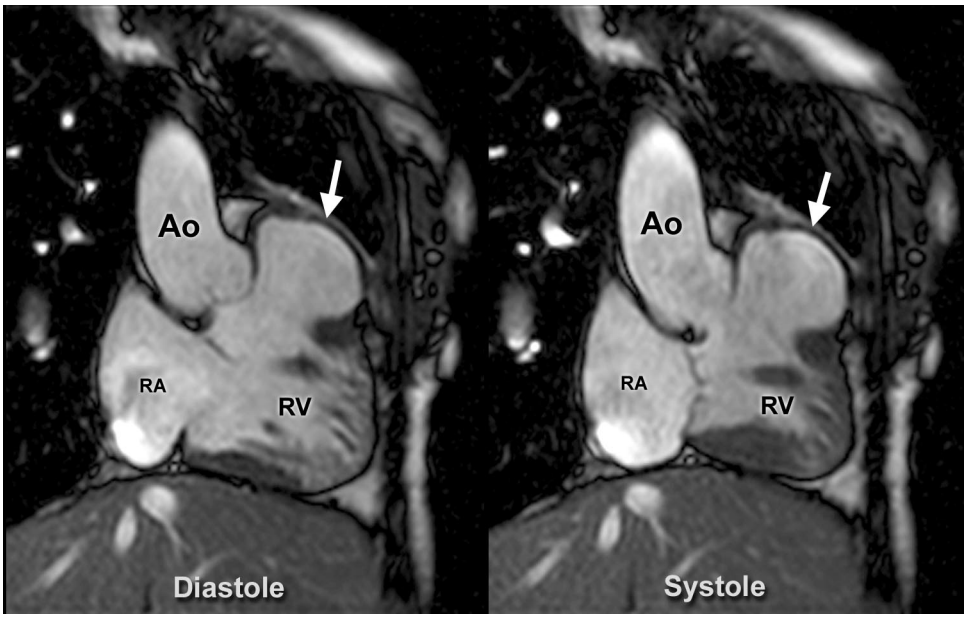

Figure 14. Dynamic cine MR images obtained along the long axis during diastole and systole show aneurysmal dilatation of a right ventricular outflow tract patch (arrow). *Ao* = aorta, *RA* = right atrium, *RV* = right ventricle.

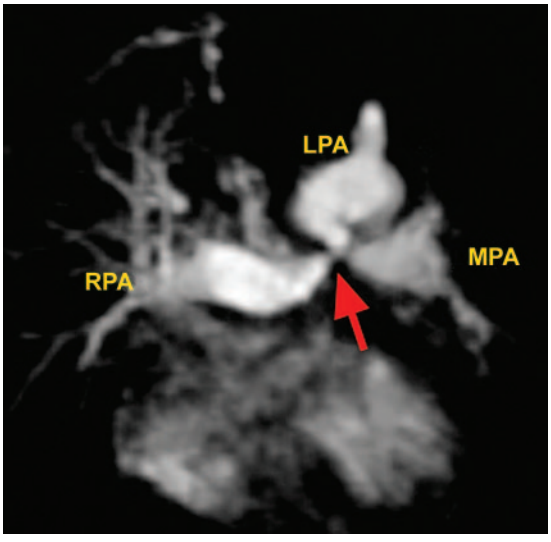

Figure 15. Coronal thick-slab reformatted MR image shows an atretic main pulmonary artery *(MPA)* segment with severe stenosis (arrow) at its junction with the left *(LPA)* and right *(RPA)* pulmonary artery branches.

Aneurysmal Dilatation of Central Shunts and Right Ventricular Outflow Tract Patches.—Occasionally, aneurysmal dilatation may develop in a central shunt, particularly in one that consists of a venous structure, because of the low resistance of the vessel wall to systemic pressure (Fig 13). For the same reason, a repair of the right ventricular outflow tract with a pericardial tissue patch may result in dilatation of the outflow tract (Fig 14).

Segmental Pulmonary Artery Stenosis.—Surgical repair early in life may not correct all existing anomalies of the segmental pulmonary vessels. Distal segments of the pulmonary arteries may remain hypoplastic and fail to grow, with resultant segmental stenosis and decreased perfusion (Figs 10, 11, 15). If the decrease is not detected in time, distal perfusion may be irreversibly compromised.

Discussion

MR has been used for noninvasive cardiac imaging for more than 10 years. Recent advances in MR imaging techniques, related to the development of both hardware and software, have led to the rapid adoption of MR imaging and MR angiography for the evaluation of complex congenital heart disease. Traditionally, congenital heart disease was diagnosed and managed with the use of echocardiography and conventional angiography, which have both advantages and limitations.

Studies have shown that MR imaging may be superior to traditional echocardiography and that it is an excellent noninvasive alternative to cineangiography because it can provide both anatomic and functional information about cardiovascular anomalies (1). In cases of tetralogy of Fallot and pulmonary stenosis, good diagnostic concordance was demonstrated between angiograms and MR images in the evaluation of right ventricular outflow obstruction. Holmqvist et al (8) reported 93% agreement with regard to a finding of main pulmonary artery stenosis, 79% agreement with regard to that of right pulmonary artery stenosis, and 86% agreement with regard to that of left pulmonary artery stenosis ($n = 14$). Agreement with regard to the finding of right ventricular enlargement was 50%; differences in assessment, in this instance, were classified as "mild" instead of "moderate" change, or as "normal" instead of "mild" change. Assessments with regard to the presence of overriding aorta and the patency and appearance of a Blalock-Taussig shunt were in agreement in 79% and 100% of cases (8).

Echocardiography is often of limited use because of a poor acoustic window due to prior thoracotomy in postoperative patients, mediastinal fibrosis, and the acoustic impedance of lung tissue (4,7,14). Beekman et al (7) concluded that MR imaging was superior to echocardiography for the evaluation of right ventricular hypertrophy and overriding aorta. In a study by Greenberg et al (17) in which echocardiography and MR imaging were directly compared in the evaluation of pulmonary abnormalities postoperatively in children with tetralogy of Fallot, MR imaging was confirmed to have greater sensitivity. Echocardiography was inadequate for depiction of the right and left pulmonary arteries in eight of 20 and in 10 of 20 children, respectively. Inadequate depiction and lack of recognition of stenosis, aneurysm, nonconfluence, and patency of hypoplastic pulmonary arteries were among the difficulties encountered (17).

Geva et al (4) compared MR imaging with conventional angiography in the evaluation of pulmonary arteries and collateral aortopulmonary vessels in 23 patients and found complete agreement between the features depicted on conventional angiograms and those depicted on MR angiograms with regard to diagnosis of hypoplasia or stenosis of a pulmonary artery branch (4).

Choe et al (18,19) evaluated whether MR imaging could depict pulmonary arterial anatomy in greater detail than routine angiography in patients with congenital or acquired occlusion of the left pulmonary artery or with pulmonary atresia. Patients in whom the pulmonary artery anatomy could not be completely identified at angiography were selected for their study. In the study group, angiography with an injection via the right ventricle or main pulmonary artery or with aortography could not be used to assess the pulmonary artery segments in these patients, as often happens in the presence of severe pulmonary artery stenosis: In seven patients, the left main pulmonary artery was not seen; in two patients with a preexistent left-sided Blalock-Taussig shunt, the hilar portions of the left pulmonary artery were not visualized; and in one patient with a prior modified right-sided Blalock-Taussig shunt, the entire pulmonary arterial tree was not depicted at angiography. In addition, the distal segments of pulmonary arteries in nine patients with unilateral pulmonary artery occlusion or discontinuity could not be identified at echocardiography. Evaluation with MR imaging was accurate in 67% percent ($n = 10$) of patients in whom pulmonary artery obstruction was proved at surgery.

Furthermore, MR velocity mapping, or right ventricular outflow measurement with the use of velocity-encoded MR images, was found superior to echocardiography in a study reported by Rebergen et al (16). Although the Bernoulli equation is used for calculation of the stenotic gradient in both techniques, the unlimited choice of imaging planes available with MR imaging allows a more accurate evaluation of the vessel dimension that is critical in the equation. MR imaging also provides a practical method of quantifying pulmonary regurgitation, as reported in the studies by Helbing and De Roos (20) and by Rebergen and colleagues (21,22).

MR imaging also has its limitations: Long acquisition times may necessitate the sedation of young children and may present a problem in the examination of patients whose clinical condition is unstable. In addition, MR imaging cannot be used in patients with an artificial pacemaker, and it cannot be used to detect abnormal calcifications in ventricular patches or coronary arteries.

Multidetector-row computed tomography is emerging as another valuable technique with fast scanning times and the capability to provide functional information (23,24). It has the disadvantage of significant radiation exposure, a factor to be considered, particularly in regard to children.

The use of echocardiography is recommended for screening and initial diagnosis and follow-up of patients with congenital heart disease. Conventional angiography should continue to be used for planning of an interventional procedure such as embolization of collateral vessels. MR imaging and MR angiography are the methods of choice for evaluating complex abnormalities and obtaining detailed anatomic and functional information without exposing the patient to ionizing radiation or the risk of an adverse reaction to iodinated contrast material. These modalities should be considered complementary rather than competitive. Further studies are needed to determine whether the use of the new noninvasive techniques improves outcomes.

Conclusions

Our review of selected examples confirms some observations reported by others and illustrates the added value and advantages of MR imaging in the evaluation of pulmonary artery anatomy in patients with tetralogy of Fallot. In most cases, cardiac MR imaging holds a distinct advantage over conventional noninvasive cardiac imaging methods such as echocardiography. Although conventional angiography remains the reference standard for evaluation of the pulmonary vasculature, contrast-enhanced MR angiography is useful as a less invasive, ionizing radiation–free method for follow-up imaging in clinically stable patients.

Evaluation of the spectrum of appearances of the pulmonary artery in tetralogy of Fallot is an excellent example of a clinically useful application of cardiac MR imaging. Important features of tetralogy of Fallot, including pulmonary artery pruning and collateral vessels, which are typically difficult to evaluate with echocardiography, are well depicted with cardiac MR imaging. Postoperative findings and complications are also better delineated with MR imaging techniques.

References

1. Mirowitz SA, Gutierrez FR, Canter CE, Vannier, MW. Tetralogy of Fallot: MR findings. Radiology 1989;171(1):207–212.
2. Van Praagh R, Van Praagh S, Nebesar RA, Muster AJ, Sinha SN, Paul MH. Tetralogy of Fallot: underdevelopment of the pulmonary infundibulum and its sequelae. Am J Cardiol 1970;26:25–33.
3. Roche KJ, Rivera R, Argilla M, et al. Assessment of vasculature using combined MRI and MR angiography. AJR Am J Roentgenol 2004;182:861–866.
4. Geva T, Greil GF, Marshall AC, Landzberg M, Powell AJ. Gadolinium-enhanced 3-dimensional magnetic resonance angiography of pulmonary blood supply in patients with complex pulmonary stenosis or atresia. Circulation 2002;106:473–478.
5. Didier D, Ratib O, Beghetti M, Oberhaensli I, Friedli B. Morphologic and functional evaluation of congenital heart disease by magnetic resonance imaging. J Magn Reson Imaging 1999;10(5):639–655.
6. Haramati LB, Glickstein JS, Issenberg HJ, Haramati N, Crooke GA. MR imaging and CT of vascular anomalies and connections in patients with congenital heart disease: significance in surgical planning. RadioGraphics 2002;22(2):337–349.
7. Beekman RP, Beek FJ, Meijboom EJ. Usefulness of MRI for the pre-operative evaluation of the pulmonary arteries in the tetralogy of Fallot. Magn Reson Imaging 1997;15(9):1005–1015.
8. Holmqvist C, Hochbergs P, Bjorkhem G, Brockstedt S, Laurin S. Pre-operative evaluation with MR in tetralogy of Fallot and pulmonary atresia with ventricular septal defects. Acta Radiol 2001; 42(1):63–69. [Published correction appears in Acta Radiol 2002;43:346.]
9. Formanek AG, Witcofski RL, D'Souza VJ, Link KM, Karstaedt N. MR imaging of the central pulmonary arterial tree in conotruncal malformation. AJR Am J Roentgenol 1986;147(6):1127–1131.
10. Donnelly LF, Higgins CB. MR imaging of conotruncal abnormalities. AJR Am J Roentgenol 1996;166(4):925–928.
11. Akins EW, Martin TD, Alexander JA, Knauf DG, Victorica BE. MR imaging of double-outlet right ventricle. AJR Am J Roentgenol 1989;152(1): 128–130.
12. Rees RS, Somerville J, Underwood SR, et al. Magnetic resonance imaging of the pulmonary arteries and their systemic connections in pulmonary atresia: comparison with angiographic and surgical findings. Br Heart J 1987;58(6):621–626.
13. Kersting-Sommerhoff BA, Sechtem UP, Higgins CB. Evaluation of blood supply by nuclear magnetic resonance imaging in patients with pulmonary atresia. J Am Coll Cardiol 1988;11(1):166–171.
14. De Roos A, Roest AA. Evaluation of congenital heart disease by magnetic resonance imaging. Eur Radiol 2000;10:2–6.

15. Soulen RL, Donner RM, Capitanio M. Postoperative evaluation of complex congenital heart disease by magnetic resonance imaging. RadioGraphics 1987;7(5):975–1000.
16. Rebergen SA, Niezen RA, Helbing WA, van der Wall EE, de Roos A. Cine gradient-echo MR imaging and MR velocity mapping in the evaluation of congenital heart disease. RadioGraphics 1996; 16(3):467–481.
17. Greenberg SB, Crisci KL, Koenig P, Robinson B, Anisman P, Russo P. Magnetic resonance imaging compared with echocardiography in the evaluation of pulmonary artery abnormalities in children with tetralogy of Fallot following palliative and corrective surgery. Pediatr Radiol 1997;27(12):932–935.
18. Choe YH, Ko JK, Lee HJ, Kang IS, Park PW, Lee YT. MR imaging of non-visualized pulmonary arteries at angiography in patients with congenital heart disease. J Korean Med Sci 1998;13(6):597–602.
19. Choe YH, Kang IS, Park SW, Lee HJ. MR imaging of congenital heart diseases in adolescents and adults. Korean J Radiol 2001;2(3):121–131.
20. Helbing WA, De Roos A. Clinical applications of cardiac magnetic resonance imaging after repair of tetralogy of Fallot. Pediatr Cardiol 2000;21(1): 70–79.
21. Rebergen SA, Chin JG, Ottenkamp J, van der Wall EE, de Roos A. Pulmonary regurgitation in the late postoperative follow-up of tetralogy of Fallot: volumetric quantitation by nuclear magnetic resonance velocity mapping. Circulation 1993; 88(5 pt 1):2257–2266.
22. Rebergen SA, Ottenkamp J, Doornbos J, van der Wall EE, Chin JG, de Roos A. Postoperative pulmonary flow dynamics after Fontan surgery: assessment with nuclear magnetic resonance velocity mapping. J Am Coll Cardiol 1993;21(1):123–131.
23. Goo HW, Park IS, Ko JK, et al. CT of congenital heart disease: normal anatomy and typical pathologic conditions. RadioGraphics 2003;23(spec issue):S147–S165.
24. Lee EY, Siegel MJ, Hildebolt CF, Gutierrez FR, Bhalla S, Fallah JH. MDCT evaluation of thoracic aortic anomalies in pediatric patients and young adults: comparison of axial, multiplanar, and 3D images. AJR Am J Roentgenol 2004;182(3): 777–784.

This article meets the criteria for 1.0 category 1 credit toward the AMA Physician's Recognition Award. To obtain credit, see www.rsna.org/education/rg_cme.html.